Proceedings of the Sixth International Conference on
Railway Technology: Research, Development and Maintenance
Edited by: J. Pombo
Civil-Comp Conferences, Volume 7, Paper 6.15
Civil-Comp Press, Edinburgh, United Kingdom, 2024
ISSN: 2753-3239, doi: 10.4203/ccc.7.6.15

Prediction of long-term damage evolution in crossing panels using an iterative simulation scheme

B. A. Pålsson[1] and U. Ossberger[2]

[1]Department of Mechanics and Maritime Sciences / CHARMEC, Chalmers University of Technology Gothenburg, Sweden
[2]voestalpine Railway Systems GmbH, Zeltweg

Abstract

This paper presents an iterative simulation methodology to compute long-term deterioration in crossing panels. The methodology takes turnout type, initial conditions and traffic load into consideration to compute the long-term change in ballast settlement and crossing geometry deterioration. The model also provides outputs in the form of structural loading such as sleeper-ballast contact pressures and bending moments in sleepers and crossing. In the methodology, the dynamic vehicle-track interaction is simulated using an MBS model with a finite element model of the crossing panel structure. To allow for computationally efficient simulation of long-term deterioration, phenomenological damage models are used. Settlements are computed using the Sato threshold model and the crossing geometry change is computed using a novel damage model derived using historical crossing geometry measurements. The methodology is demonstrated for a switch & crossing demonstrator installed in the Austrian railway network as a part of the European research programme Shift2Rail, and the measured crossing geometry change after 26 months of traffic is compared to model predictions.

Keywords: crossing, turnout, measurements, multibody simulations, dynamic vehicle-track interaction, calibration

1 Introduction

A so-called Whole System Model (WSM) for railway switches and crossings (S&C, turnouts) is developed within the European research programme Shift2Rail and its

In2Track projects [1]. The objective is that this type of model should allow for holistic simulation-based assessment of S&C designs. In the WSM, dynamic interaction between S&C and passing vehicles is considered along with the loading and deterioration of S&C components over time. An iterative approach is applied where damage increments are computed and accumulated in the model for increments of traffic loading. Given the vast differences in length and time scales involved in dynamic vehicle-track interaction compared to long-term track degradation, it is not feasible for a single model to capture all relevant aspects of long-term S&C deterioration and performance. The WSM is therefore a framework that integrates state-of-the-art simulation tools and techniques. Depending on the objectives of a given study, the WSM scheme can be tailored for the current task. For the present investigations the focus lies on crossing geometry change, ballast settlement and the related changes in structural loading. A schematic representation of this WSM is presented in Figure 1.

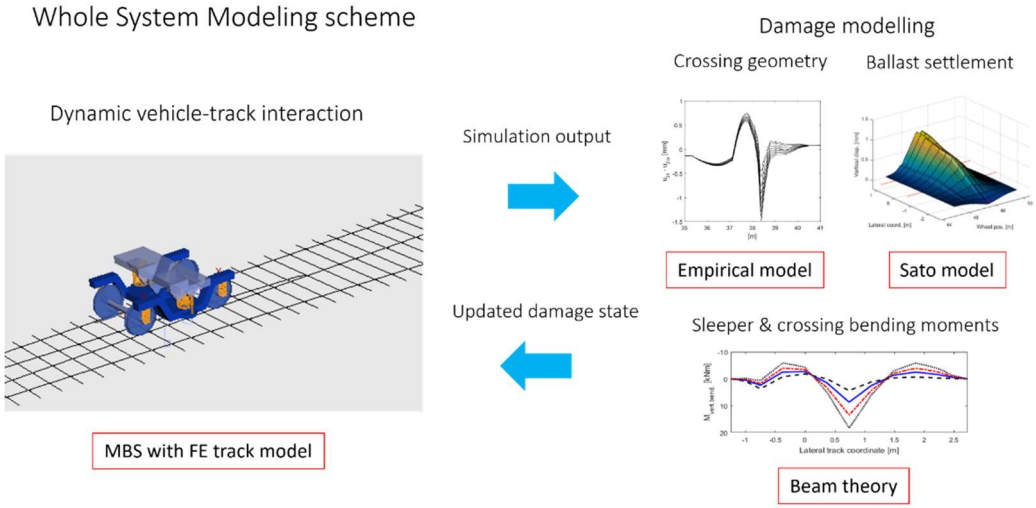

Figure 1: Schematic illustration of the present version of the Whole System modelling scheme.

While the literature contains several demonstrations of iterative schemes that compute accumulated damage in S&C for switch panels [2], crossing panels [3,4] and ballast [5], the WSM considers simultaneous deterioration in multiple damage modes allowing for the study of interaction between damage mechanisms [6]. This makes the WSM useful for the evaluation of different maintenance regimes in addition to design studies.

The first demonstration of the WSM [6] used the multibody simulation model from the switches and crossings simulation benchmark [7] with a co-running track model to simulate the dynamic-vehicle track interaction, and then used a phenomenological model to study the ballast settlement rate and the crossing damage modelling in [4] to predict crossing deterioration in the form of plastic deformation and wear using Archard's wear law and detailed FE-calculations of cross-sections in the crossing nose. Based on the experiences from this WSM demonstration, it was concluded that the model could benefit from a FE-type track model to allow for the direct extraction

of structural loading and sleeper-ballast contact pressure. It was also concluded that the crossing damage model is cumbersome to apply as the simulation times are counted in weeks for studies involving multiple Mega Gross Tonnes (MGT). The present paper has therefore aimed to improve the WSM scheme in these two areas.

This version of the WSM uses the model from [8] for MBS simulations, which has been calibrated to the S2R S&C demonstrator. It also uses a novel hybrid model to compute crossing geometry change and a threshold model from [9], originally developed by Sato, for ballast settlement calculations. This type of MBS model allows for the extraction of physical responses in the track structure in the form of nodal displacements. These can in turn be used to compute the structural loading in the form of loads in rails and sleepers due to bending, as well as sleeper-ballast contact pressures. The crossing damage model is empirical and has been derived using data from a long-term measurement series of a previously studied crossing in the Austrian network [4], in order to derive geometry deterioration modes and damage sensitivities, while the damage propagation rate in simulation is determined by the simulated impact loading.

The studied S&C is a 60E1-500-1:12 demonstrator installed in the Austrian network as a part of the In2Track projects that are part of the EU-sponsored Shift2Rail research programme. It is built from 60E1 rails, has a nominal radius of 500 metres and a turnout angle of 1:12. The S&C is located between Vienna and Liesing and is situated in a track section with a radius of 3500 m. See Figure 2 for pictures. The demonstrator features novel developments compared to a standard design: it uses a soft rail fastening system, under sleeper pads, a new crossing rail design and a sleeper design with a wider base towards the ends for increased ballast support. The properties of the crossing panel are presented further in the modelling section. The actual demonstrator is a left-hand S&C while the continued presentation will be mirrored to a right-hand S&C to match the modelling and simulation environment.

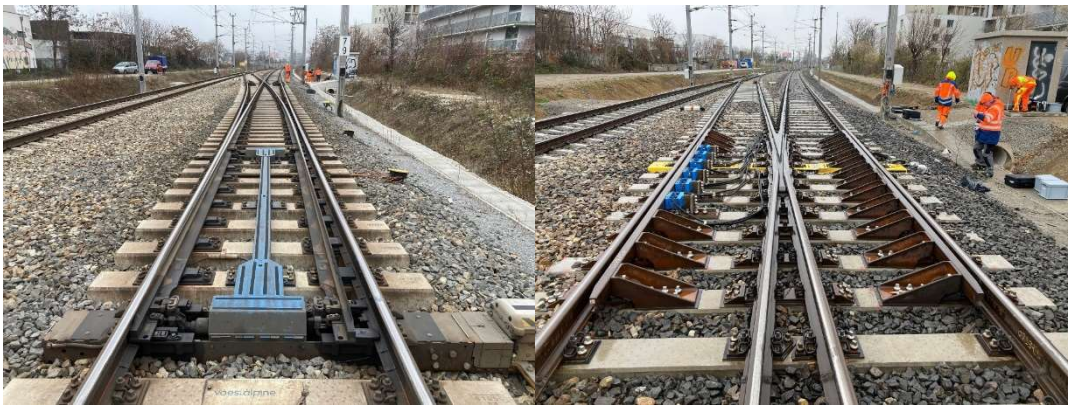

Figure 2: Pictures from the demonstrator test site taken by voestalpine Railway Systems GmbH. The whole S&C seen from the switch panel side (left) and detail of the crossing panel (right). Through route to the right and diverging route to the left in both pictures

The crossing rail geometry was measured at several discrete cross-sections using a CALIPRI laser scanning device [10]. The section spacing was 50 mm in the transition area of the crossing. The measured geometry has been trimmed of excessive data to only leave the geometry relevant to represent the running surface. In Simpack, the wing rail and the crossing rail are implemented as separate wheel-rail contact definitions defined by their measured discrete cross-sections. These 3D rail profile shapes are then generated via longitudinal spline interpolation, while the running surface of the stock rails and check rails are modelled using their nominal profiles. For the present investigation, two geometry measurements are used, one from the new crossing and one after 26 months of traffic. The cross-sections for the new crossing are presented in Figure 3.

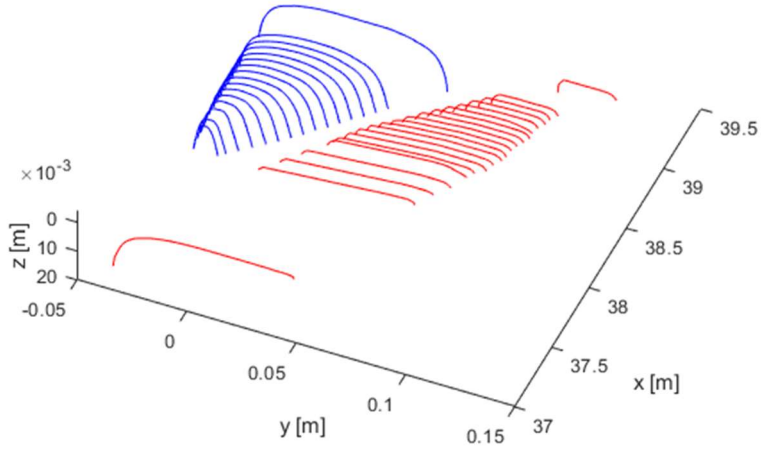

Figure 3: Rail cross-sections for wing rail (right) and crossing nose (left) in the rail's local coordinate system.

2 Simulation model

For the present investigation, the MBS model consists of a ½ vehicle model, i.e. a bogie with half of the car body mass on top, and a finite element model representation of the crossing panel, see Figure 4. The vehicle and track models are truncated to save computational effort as the crossing transition is the primary focus. Here the length of the track model is 22 m. In [11], a convergence study was performed for a similar simulation case and it was shown that this track model length is sufficient and does not have any significant influence from the rail boundaries at the crossing transition. The model is initiated by finding the static equilibrium for each evaluated track configuration before the start of the time-domain simulation.

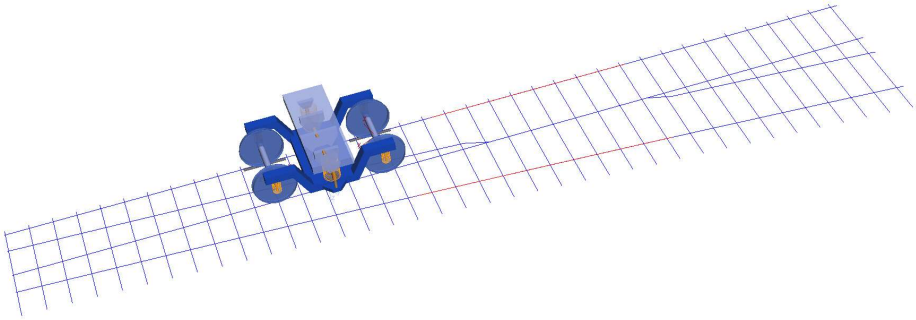

Figure 4: Illustration of crossing panel with bogie train model. Blue lines represent the track structure in the form of rails and sleepers. Red lines indicate check rails.

The track model is a two-layer finite element model where rails and sleepers are modelled with Timoshenko beam elements. The rail fastenings are represented with linear Kelvin bushing elements consisting of linear springs and dampers. The ballast and subgrade is represented by bi-linear springs in the vertical direction to represent potential voids between ballast and sleeper. The damping is modelled using linear viscoelasticity and is therefore active also when there is a gap. The track model of the crossing panel is implemented in the MBS code Simpack [12] using its *non-linear flextrack* module. The track model is generated using a Matlab [13] script that generates the necessary input bodies, bushing elements and track definition (.ftr) file for Simpack. Full details on the track model in terms of modelling, properties and calibration to the S2R demonstrator can be found in [8].

To represent the traffic load, the ½ vehicle model based on the Manchester benchmark passenger vehicle [14] was adjusted to correspond to a ER20 locomotive axle load (20 tonnes) and bogie wheelbase (2.7 m). The vertical suspension properties were adjusted in proportion to the increase in car body mass to maintain resonance frequencies. A nominal S1002 wheel profile was used in the simulations. This is the same vehicle model that was used for train run tests at the S2R demonstrators and that were used for calibration of the track model. The same vehicle model was therefore kept for comparability.

3 Damage modeling

To allow for the simulation of long-term crossing geometry deterioration at a low computational cost, an empirical modelling approach is applied where damage rates and modes for the longitudinal profiles of wing rail and crossing nose are derived using measurement data. The data in this case comes from a long-term measurement series of a crossing in the Austrian network using data analysis and supporting simulations. The crossing geometry measurement series consist of 12 consecutive geometry measurements that cover 0 to 65 MGT of traffic. As this crossing was located in a S&C where also the main route is curved, it saw higher deterioration rates than a comparable crossing located in a straight through route. The measurements are

combined with simulation results from [15] as well as novel analysis to estimate the influence of impact load levels on deterioration rates.

By studying the point of maximum geometry change in the crossing over time, it was found that the geometry change magnitude of the reference crossing (d_{ref}) as a function of axle passages (N) can be expressed well with Equation (1). The *ln*-term captures the non-linear hardening behaviour of the crossing material as well as the profile geometry change that reduces the contact pressures, and the linear term captures the wear that typically grows with a fairly constant rate over time [4].

$$d_{\mathrm{ref}}(N) = k_1 \ln(k_2 N + 1) + k_3 N \tag{1}$$

The geometry change rate for the reference case can then be obtained by computing the derivative of (1) in Equation (2) as

$$\frac{\partial d_{\mathrm{ref}}(N)}{\partial N} = \frac{k_1 k_2}{k_2 N + 1} + k_3 \tag{2}$$

In order to scale this rate of change to novel operating conditions with different wheel-rail contact loads, a scale factor was derived according to Equation (3). It relates the Q-force level in simulation (Q), to the estimated forces experienced by the measured crossing as a function of axle passages, $Q_0(N)$. In simulations the representative Q-force is computed as the peak value of the Q-force signal that has been low-pass filtered at 250 Hz. A calibration factor C is also added to account for other differences in running conditions between different crossings.

$$g(N, Q) = C \frac{Q}{Q_0(N)} = C \left(\frac{k_4 Q}{k_5 N + m_2} - m_1 \right) \tag{3}$$

The scale factor was derived by simulating the measured crossing geometries scaled for 1:12, 1:15 and 1:18.5 crossing angles and comparing the impact load levels to the simulated deterioration rates for the same cases from [15]. The scaled damage curve is then obtained by multiplying the functions according to Equation (4)

$$d = g(N, Q) d_{\mathrm{ref}}(N) \tag{4}$$

To get the damage rate for the combined function, the product derivative is computed in Equation (5), but as the partial derivative of $g(N, Q)$ with respect to N was found to be negligible the equation can be simplified.

$$\frac{\partial d}{\partial N} = \frac{\partial g(N, Q)}{\partial N} d_{\mathrm{ref}}(N) + g(N, Q) \frac{\partial d_{\mathrm{ref}}(N)}{\partial N} \approx g(N, Q) \frac{\partial d_{\mathrm{ref}}(N)}{\partial N} \tag{5}$$

The magnitude of crossing geometry change in each step of the methodology for the observed force level Q is then computed according to Equation (5). The crossing geometry change is then introduced by changing the vertical positions of the wing rail and crossing nose cross-section profiles according to the geometry change times basis functions derived from the measurement series. Basis functions of the deterioration can be used with good accuracy as the deterioration patterns are close to uniform over time. Numerical values for all constants are: $k_1 = 24e-3\ [m]$, $k_2 = 1/12500$ [-], $k_3 = 43e-9\ [m]$, $k_4 = 1.64e-3\ [-]$, $k_5 = 8.2e-3[N]$, $m_1 = 0.67\ [-]$ and $m_2 = 177e3\ [N]$.

The ballast settlement model is a truncated version of the threshold model from [16] originally developed by Sato. The non-linear term is omitted as its influence is negligible for the ballast pressure magnitudes present in this study. The model predicts a settlement that is proportional to pressures that exceed a threshold. The settlement propagation coefficient is 1.33 e-8 [m/Pa] per 10 000 loading cycles as in [16] while the pressure threshold for settlement is taken as 85kPa. The ballast settlement model is time-invariant as the propagation coefficient and settlement threshold are constant in time. The model therefore does not account for any change in ballast quality over time.

4 Iterative scheme

In each step of the iterative scheme, the dynamic vehicle-S&C interaction is simulated using the MBS model followed by the calculation of a damage increment from the track response. The damage increment is added to the MBS model before the next step and so the iterative scheme continues until the end of simulations. The nominal iteration step corresponds to a few MGT of traffic. The iteration step is reduced if necessary to cap the maximum settlement increment to 0.1 mm to avoid numerical instabilities. The iteration scheme is applied to simulate accumulated damage from the calibrated state of the S2R S&C demonstrator with and without the identified sleeper voids to compare the long-term response of the crossing panel for these two cases. The simulation methodology took around six hours to simulate the 26 months of traffic between crossing geometry measurements using 42 iteration steps. Initial simulations showed that the derived damage curve for the crossing overestimated the crossing damage rate. The calibration factor C in Equation (3) was therefore reduced by 25% to 0.75 to obtain agreement with the measured deterioration rates.

5 Results

Figure 5 shows the relative vertical wheel-rail displacement (kinematic motion) as a wheel roll over the crossing transition and the corresponding vertical contact forces.

Results are given for the measured crossing geometries as well as for crossing predicted by the model using the calibration factor 0.75. It can be observed that both the kinematic motion and the force levels are similar for the measured and predicted crossings even though there are minor variations that can be expected as the deformation modes in the model are taken from another crossing.

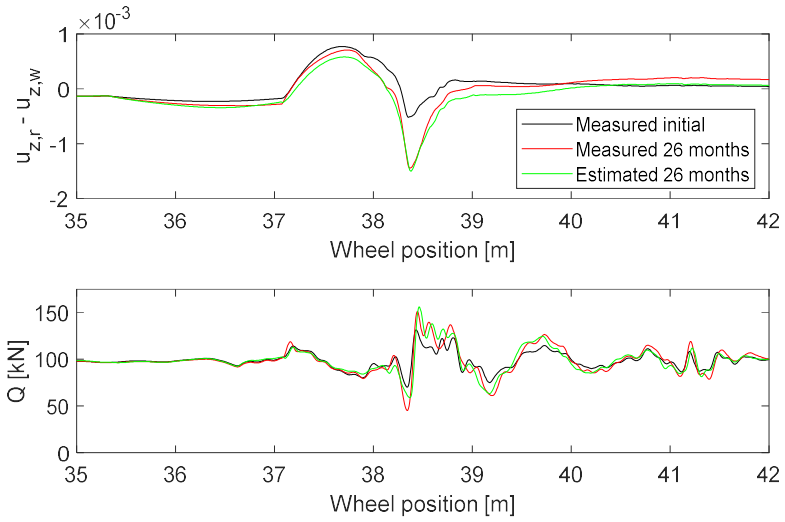

Figure 5: Top: Relative vertical movement between wheel and rail describing the dip at the crossing transition. Bottom: Vertical wheel-rail contact force. The wheel's wing rail to crossing nose transition is located at around 38.3 m

Figure 6 plots a set of selected responses as a function of time for the S2R demonstrator with and without voids under the crossing sleeper. Each plotted quantity is described in Table 1. It can be concluded from the figure that the uneven ballast distribution increases structural loading in terms of bending moments in sleepers and crossing and increase track deflection. The dynamic wheel-rail contact forces on the other hand are not affected by the small ballast voids in the present study. Throughout the studied period, the maximum sleeper-ballast contact pressure is located at the field side of the crossing panel as it is tilting slightly to one side under the train load. This phenomenon is illustrated in Figure 7 that shows the calibrated void distribution at the start of simulation and after 26 months using the assumed ballast settlement threshold. Even though the exact threshold value for settlements is unknown, the figure clearly indicates the region of the higher sleeper-ballast contact pressure.

Quantity	Description
Maximum bending moment crossing ($M_{\max}$)	The maximum bending moment anywhere in the crossing
Maximum bending moment sleeper ($M_{\max}$)	The maximum bending moment anywhere in the sleeper under the crossing transition
Crossing $u_{\max}$ at transition	The maximum displacement in the crossing at the wing rail to crossing transition
Sleeper $u_{\max}$ at crossing	The maximum displacement in the sleeper at the wing rail to crossing transition at the crossing rail seat
Sleeper $p_{\max}$	The maximum sleeper-ballast contact pressure anywhere under the crossing at the wing rail to crossing transition
Sleeper $p_{\max}$ at crossing transition	The maximum sleeper-ballast contact pressure under the crossing transition.
$Q_{\max}$ filt 1250 Hz	Maximum vertical impact load at the crossing transition after the force signal has been low-pass filtered at 1250 Hz.
$Q_{\max}$ filt 250 Hz	Maximum vertical impact load at the crossing transition after the force signal has been low-pass filtered at 250 Hz.

Table 1. Description of plot quantities in Figure 6. All quantities are derived from simulation outputs from the passage of the leading axle in the bogie.

6 Conclusions

An iterative scheme to predict long-term damage evolution in crossing panels has been presented and the crossing deterioration after 26 months of traffic has been compared to measurements from the S2R demonstrator. It has been shown that the empirically derived crossing damage model can give a good estimate of the crossing geometry deterioration also in a novel setting, even though a reduction in damage rate of 25% was required to get perfect agreement. The prediction accuracy of the model can most likely improve if more measurement data can be used in the derivation of the model.

Studying the sleeper-ballast contact pressures it can be concluded that the highest pressures were found at the field side of the crossing panel and not under the crossing for the studied time duration, i.e. also with a slightly worn crossing.

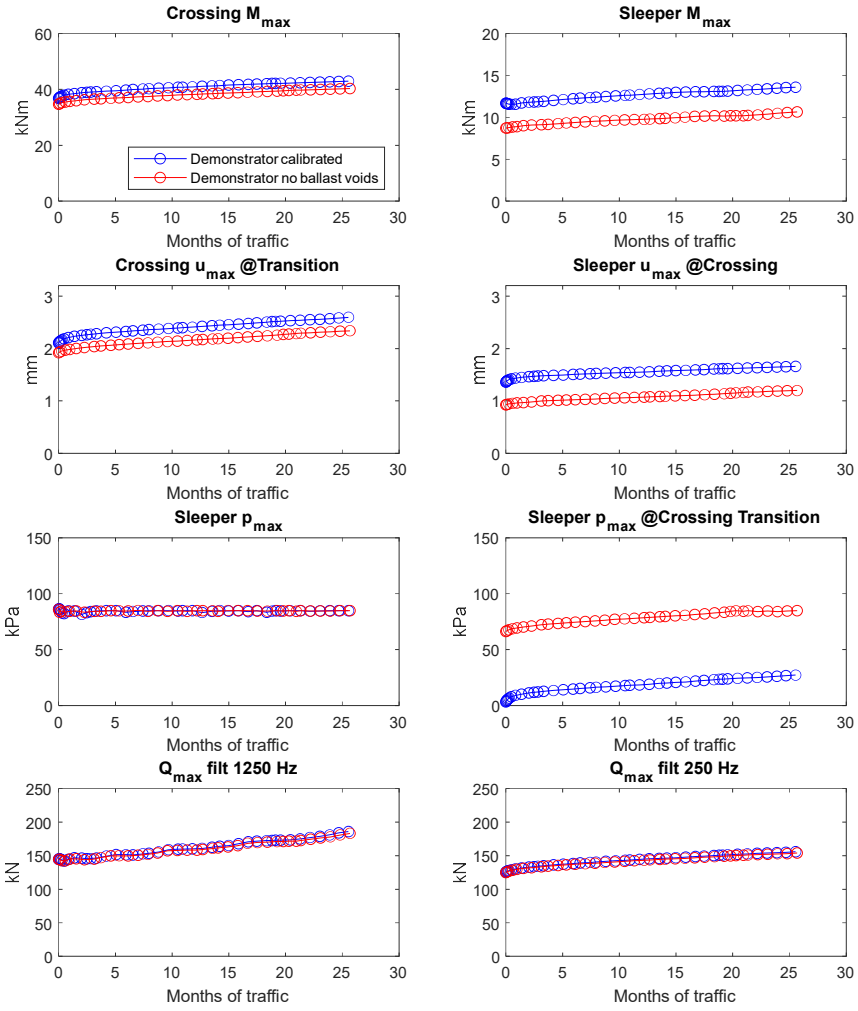

Figure 6: Evolution of structural responses and loads over time. See Table 1 for description of each quantity.

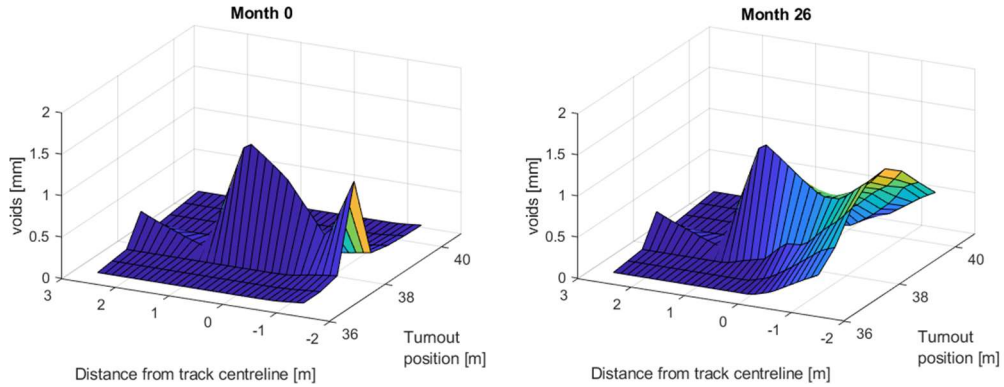

Figure 7. Ballast void distribution in the crossing panel. Left: The calibrated ballast void distribution at Month 0 from [8]. Right: The simulated ballast void distribution at month 26.

Acknowledgements

The current study is part of the on-going activities in CHARMEC (Chalmers Railway Mechanics, www.chalmers.se/charmec). Parts of the study have been funded within the European Union's Horizon 2020 research and innovation programme in the Shift2Rail project In2Track3 under grant agreement 101012456.

References

[1] In2Track, "Deliverable 2.2 Enhanced S&C Whole System Analysis, Design and Virtual Validation (final)", 2020.

[2] P. Wang, J.M. Xu, K.Z. Xie et al. "Numerical simulation of rail profiles evolution in the switch panel of a railway turnout", Wear 366-367, 105-115, 2016.

[3] A. Johansson, B. Pålsson, M. Ekh et al, "Simulation of wheel-rail contact and damage in switches & crossings", Wear 271(1-2), 472-481, 2011.

[4] R. Skrypnyk, U. Ossberger, B.A. Pålsson et al, "Long-term rail profile damage in a railway crossing: Field measurements and numerical simulations", Wear 472, 2021.

[5] X. Li, M. Ekh, J.C.O. Nielsen, "Three-dimensional modelling of differential railway track settlement using a cycle domain constitutive model", Int J Numer Anal Meth Geomech, 40, 1758-1770, 2016.

[6] K. Six, K. Sazgetdinov, N. Kumar et al, "A whole system model framework to predict damage in turnouts", Vehicle Syst Dyn 61(3), 871-891, 2021.

[7] Y. Bezin, B.A. Pålsson, "Multibody simulation benchmark for dynamic vehicle-track interaction in switches and crossings: modelling description and simulation tasks", Vehicle Syst Dyn 61(3), 644-659, 2021.

[8] B. Pålsson, H. Vilhelmson, U. Ossberger et al, "Dynamic vehicle–track interaction and structural loading in a crossing panel – Comprehensive field measurements and calibration of a simulation model", Vehicle Syst Dyn, 1-27, 2024, https://doi.org/10.1080/00423114.2024.2305289

[9] X. Li, J.C.O. Nielsen, B.A. Pålsson, "Simulation of track settlement in railway turnouts" Vehicle Syst Dyn 52, 421-439, 2014.

10. CALIPRI C4X measurement device. Available from: https://www.nextsense-worldwide.com/en/

[11] M.D.G. Milosevic, B.A. Pålsson, A. Nissen et al, "Reconstruction of sleeper displacements from measured accelerations for model-based condition monitoring of railway crossing panels", MSSP 192:1-21, 2023.

[12] Simpack. Version 2022x.4: Dassault Systemes; 2022. Available from: 3ds.com

[13] Matlab R2021. The Matworks Inc.

[14] S. Iwnicki, "Manchester benchmarks for rail vehicle simulation", Vehicle Syst Dyn 30(3-4), 295-313, 1998.

[15] R. Skrypnyk, B.A. Pålsson, J.C.O. Nielsen et al. ”On the influence of crossing angle on long-term rail damage evolution in railway crossings”, Int J Rail Transp 9(6), 503-519, 2021.

[16] X. Li, J.C.O. Nielsen, B.A. Pålsson, “Simulation of track settlement in railway turnouts” Vehicle Syst Dyn 52, 421-439, 2014.